Multistatic Wireless Fidelity Network Based Radar: Results of the Chrcynno Experiment

Stanisław RZEWUSKI, Maciej WIELGO, Karol KLINCEWICZ, Łukasz PODKALICKI, Krzysztof KULPA, Mateusz MALANOWSKI

Inst. of Electronic Systems, Warsaw University of Technology, ul. Nowowiejska 15/19, 00-665 Warsaw, Poland

srzewuski@mion.elka.pw.edu.pl, mwielgo@mion.elka.pw.edu.pl, kklincewicz@mion.elka.pw.edu.pl, lukasz@sabalisystems.com, kulpa@ise.pw.edu.pl, m.malanowski@elka.pw.edu.pl

Abstract. *This paper presents the theory and experimental result of passive radar using WIFI transmitters as illuminators of opportunity. As a result of experiments conducted on 17th August 2013 at airfield Chrcynno a Cessna C208 airplane was detected using multistatic passive radar system based on low power signal from WIFI network nodes, which were acting as non-cooperative illuminators of opportunity. In the experiment the 3 wireless access points (AP) were communicating with each other and illuminating the radar scene (airfield). The direct reference and reflected (surveillance) signals have been acquired and processed using specially developed algorithm presented in the paper. After signal processing using Passive Coherent Location methods the target has been detected. This paper describes in details the algorithms and the results of the experiment for the multistatic passive radar based on the WIFI signal.*

Keywords

Passive radar systems, passive coherent location, passive bistatic radar, multistatic passive radio location, noise radars, WIFI signal decoding, frame detection, processing signal from wireless networks.

1. Introduction

The passive radar, in contrast to the active one, does not emit electromagnetic energy but harvests energy originated from commercial communication transmitters. The first passive radar demonstrator was itspresented and tested during the Daventry experiment in February 1935. It used BBC short wave radio transmitter as the source of the target illumination. The idea of the passive radar is not very new, however recently it has been having its renaissance because many different widely used radio telecommunication systems exist in the environment. This gives an excellent opportunity to use them as illuminating sources for new passive radar systems.

The selection of the illuminator of opportunity depends on the required performance of the passive radar. The best detection range can be achieved by using strong (up to 100 kW) FM radio transmitters, but due to the small bandwidth the range resolution is very poor (worse than 1 km) and content dependent [15], [16]. The DVB-T illuminators can have also up to 100 kW power and almost 8 MHz bandwidth giving good range resolution and long detection range [10]. Other emitters like GSM [9], 3G, LTE, WiMax and WIFI are used less often as the detection ranges are much shorter. Some of them, however, give a chance to improve the range resolution due to the larger bandwidth.

In Qifan Pu paper [6] one can see that even the human gesture tracking using WIFI illuminator is possible. The WIFI radiolink world record (382 km) has been set in 2007 in Venezuela by Ermanno Pietrosemoli [7]. Such a long distance radiolinks can be used for detecting objects flying in the region between the antennas of the radio line. During such a detection, a forward scattering problem has to be solved (object creates interferences in reference signal). The issue of forward scattering has been described in [8]. One can see very large potential in WIFI based passive radars and sensors.

This paper presents the passive radar using WIFI signal as a source of the target illumination. The demonstrator named WIFIRAD was constructed at Warsaw University of Technology. The signal that is processed by WIFIRAD has following parameters:

1. The compatibility with IEEE 802.11g standard.
2. 2.4 GHz carrier frequency.
3. OFDM modulation standard.
4. Transmission bandwidth of 6Mbps.
5. Channel width 20 MHz (the signal was recorded with span 36 MHz).

Currently using WIFIRAD it was possible to detect moving cars in monostatic (transmitter and receiver are collocated) [3], [4] and bistatic [5] (transmitter and receiver are separated) configuration. In the experiments range between the radar and detected target was varying from 70 m to 300 m. In this paper the results of full multistatic configuration are presented, where multiple spatially separated transmitters are used. The paper is focused in the target detection and localization. The target tracking is out of the scope of the paper.

The rest of the paper is organized as follows: in Section 2 the structure and properties of illuminating signal are presented. In Section 3 the theoretical analyses and the properties of multistatic passive radar are presented. In Section 4 the Chrcynno (52°34′33″N 20°52′23″E) experiment is described in the details showing the signal processing algorithms and the results of the experiment.

2. Illuminating Signal Structure

The WIFIRAD passive radar demonstrator is using WIFI signals of opportunity for target illumination. The WIFI transmitters operate in the 2.4 GHz band. The signal bandwidth of the single illuminator is equal to 20 MHz. It is assumed that all the illuminators in the area are using the same frequency channel, thus the passive radar receiver minimal bandwidth is also equal to 20 MHz. The range resolution in such a case reaches the value of 7.5 m, assuming quasi-monostatic configuration (see formula 4 in Section 3.1). While all the transmitters share the same frequency channel, it is necessary to recognize during the processing the illuminating station for each successive illumination (transmitted frame). This is essential during target localization, as the precise geometry has to be known. To perform this action it is necessary to find the transmitter identification using the knowledge of the signal structure.

WIFI uses time multiplexing transmission with OFDM (Orthogonal Frequency Division Multiplexing) modulation. The WIFI signal in time and frequency domain is presented in Fig. 1. and Fig. 2.

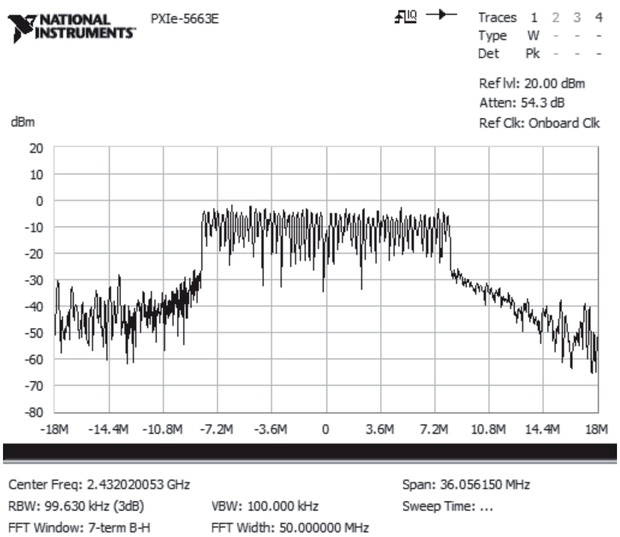

Fig. 1. The spectrum of WIFI signal measured using NI - RFSA equipment. Vertical axis power in dBm, horizontal axis MHz.

The frame structure of the transmitted signal is presented in Fig. 3. The frame consists of the three main parts: Physical Layer Convergence Procedure Preamble (PLCP Preamble), SIGNAL and the DATA. PLCP Preamble field is used to synchronize the receiver with training sequence. The SIGNAL field contains all the information of the PLCP HEADER except SERVICE which is a part of the DATA field. SIGNAL is coded using BPSK (Binary Phase Shift Keying) modulation with the rate of $R = 1/2$ and it forms a single OFDM symbol. The SIGNAL field is divided into: RATE field that carries information about the type of modulation and the coding rate used for DATA field. LENGTH field determines the number of octets that will be transmitted in the frame.

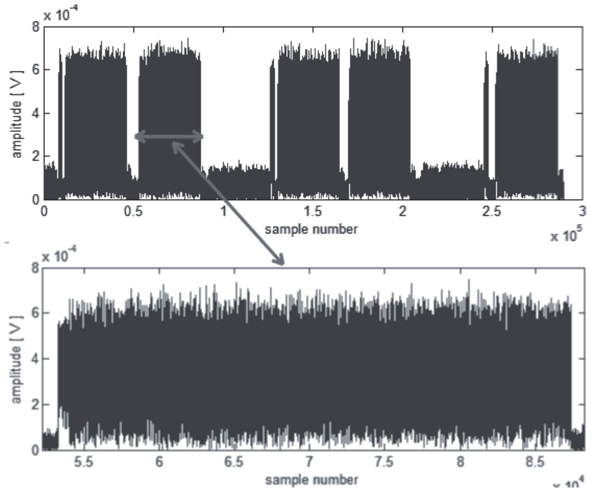

Fig. 2. WIFI network frames in time domain (upper image) and single frame (lower image). Horizontal axis sample number, vertical axis amplitude.

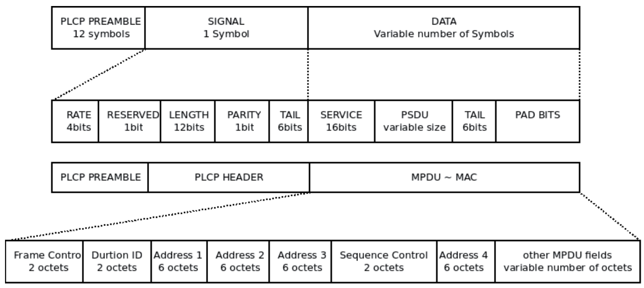

Fig. 3. WIFI frame structure.

PARITY bit is an even parity for all preceding bits; All TAIL bits are set to zero. DATA field includes the last part of PLCP Header (SERVICE field), MAC protocol data unit (MPDU), DATA TAIL and PAD BITS. SERVICE contains the information about the scrambler initialization, which is important for signal decoding. DATA TAIL bits are set to zero. DATA field consists of more than one OFDM symbols. PAD BITS are added to ensure that the number of bits in the DATA field will be a multiple of number of coded bits per symbol. The most important information for WIFIRAD passive radar systems is inside MPDU. The most interesting fields are Address 1, 2, 3, and Address 4. Depending on the Frame type they contain the following information: Basic Service Set Identifier (BSSID), SOURCE ADDRESS, DESTINATION ADDRESS, Transmitting STA (station) address and receiving STA (station) address. BSSID identifies Basic Service Set (BSS) and defines the wireless network name on given area. Knowing SOURCE ADDRESS value it is possible to determine the source of the signal transmission out of whole wireless network signals. This information is used for signal separation in WIFIRAD signal processing algorithms, as described in Section 4.1.

3. Fundamentals of Bistatic Passive Radar

The WIFIRAD experiment presented in this paper is done in multistatic configuration that consists of 3 access points (AP's) and the radar receiver. Each single AP and the radar receiver form a bistatic configuration. In the experiment there were three such AP-radar pairs. In this section the basic fundamentals of single bistatic transmitter-receiver pair will be described.

The idea of passive radar is presented in Fig. 4. The transmitter of opportunity (AP) illuminates both the target and the radar. The radar is equipped with two receiving channels. One is dedicated to receiving the reference (illuminating) signal while the second is used as surveillance channel receiving target echo. The target echo signal is shifted in time (due to the longer propagation path) and frequency (due to the Doppler effect). These shifts define the bistatic range and bistatic velocity of the target. To compute them, the crossambiguity function (described in details in Section 3.1) is used.

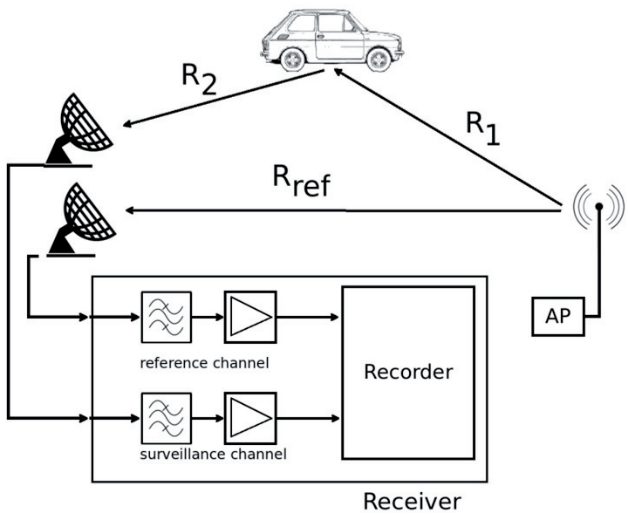

Fig. 4. Simplified bistatic passive radar scenario.

As stated above the received echo signal is shifted in time with respect to the reference signal by the value

$$\tau = \frac{R_1 + R_2 - R_{\text{ref}}}{c} \tag{1}$$

where R_1 – the distance between the transmitter and the target, R_2 – the distance between the target and the radar, R_{ref} – the distance between the transmitter and the radar, τ – the time shift, c – the speed of light.

The bistatic range R_B, is defined as:

$$R_B = R_1 + R_2 - R_{\text{ref}} \, . \tag{2}$$

The received echo signal is also frequency shifted with respect to the reference signal due to the Doppler effect. The Doppler frequency shift is related to the bistatic velocity v_B using the following formula:

$$f_d = \frac{v_B f_c}{c} \tag{3}$$

where f_C is carrier frequency, f_d is Doppler frequency offset c is speed of light ,v_B is bistatic velocity.

The bistatic velocity is the derivative in time of the bistatic range (2) and can be defined as in formula (4):

$$v_B = \frac{\mathrm{d}R_B}{\mathrm{d}t} \tag{4}$$

The bistatic velocity can be thus calculated knowing the target velocity vector v as a sum of projection of that vector on two versors u_1 and u_2 presented in Fig. 5, using the following formula:

$$v \cdot u_1 + v \cdot u_2 = \mathrm{v}_B \tag{5}$$

where v is the object velocity vector, u_1 is the versor from object towards receiver Rx, u_2 is the versor from object towards transmitter Tx, ($\cdot$ denotes dot product).

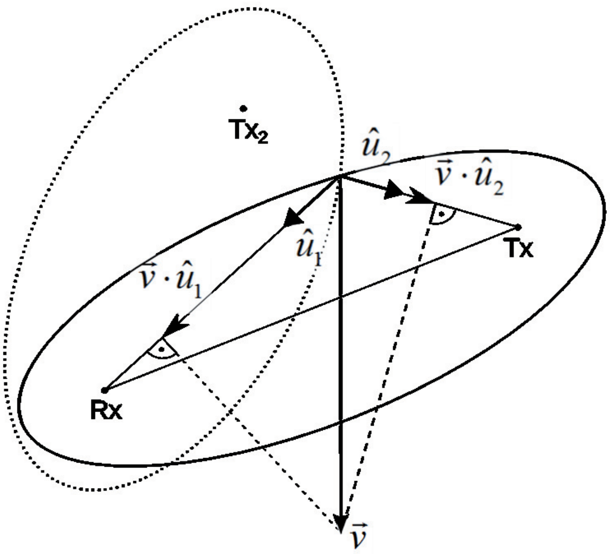

Fig. 5. Geometry illustrating the relationships of velocity vectors.

In case of the measurement based on a single receiver-transmitter pair the location of the object is unknown and u_1 and u_2- versors cannot be determined. When two more transmitter receiver pairs are used (minimum 2 in 2-D case or 3 in 3-D case) it is possible to localize target by finding ellipsoid crossing and determining the velocity vector v knowing Doppler shift of signals, as depicted in Fig. 5.

3.1 Crossambiguity Function

The detection in passive radar is based on the matched filter concept equivalent to the concept of correlation processing. If the bistatic range and velocity is known, the optimal (in the mean square sense) detector can be constructed by calculating complex correlation between received signal and time- and the Doppler-shifted copy of reference signal. In practical case, when target position and velocity is unknown, it is necessary to calculate the values of correlation function for all the possible bistatic ranges and velocities under consideration. It is equivalent to the calculation of a cross-ambiguity function between the received and the reference signal (6):

$$y(R_B, v_B) = \int_{t=0}^{T_i} x_R(t) x_T\left(t - \frac{R_B}{c}\right) e^{-j2\pi\frac{v_B f_c}{c}t} dt \qquad (6)$$

where R_B is the difference between target-receiver and target-radar distances, v_B is the bistatic velocity, f_C is carrier frequency, c is speed of light, t is time, T_i is integration time, x_R is the received signal, x_T is the transmitted signal.

The precision of the information extracted from the crossambiguity function has some limitations due to the signal bandwidth and integration time. The WIFIRAD passive radar uses WIFI networks signal that has 20 MHz channel bandwidth. The bistatic range resolution (in quasi-monostatic case) is equal to 7.5 m and can be calculated from formula (7):

$$\Delta R = \frac{c}{2B} \qquad (7)$$

where ΔR is the bistatic resolution of a radar system [m], c is the speed of light [m/s], B is the bandwidth of a radar system [Hz].

The Doppler resolution can be estimated from (8):

$$\Delta f = \frac{1}{T_i} \qquad (8)$$

where Δf is Doppler resolution [Hz], T_i is integration time [s].

The integration time has to be long enough to provide sufficient Doppler resolution and sensitivity of the radar (longer integration time provides more integration gain), but is limited by target motion - target should stay in a single range and velocity resolution cell during integration time.

Before the experiment, the ambiguity function of the WIFI signal has been calculated to analyze its character. More details about it along with the theoretical analysis have been published in [4]. The ambiguity function of the signal that was used as the reference signal in the experiment is presented in Fig. 6. Since the character of the ambiguity function was known, the analysis of the crossambiguity function becomes more straightforward. On the ambiguity function in Fig. 6 one can see additional local maxima apart from the peak at zero range and zero velocity. These local maxima are caused by the cyclic prefix presence in the signal. They occur in a distance that corresponds to OFDM symbol length, which is 3.2 µs.

The WIFI transmission has a packet character causing Doppler spread of ambiguity function, clearly visible in Fig. 6. Traffic density can vary in time. Duty factor F_u is

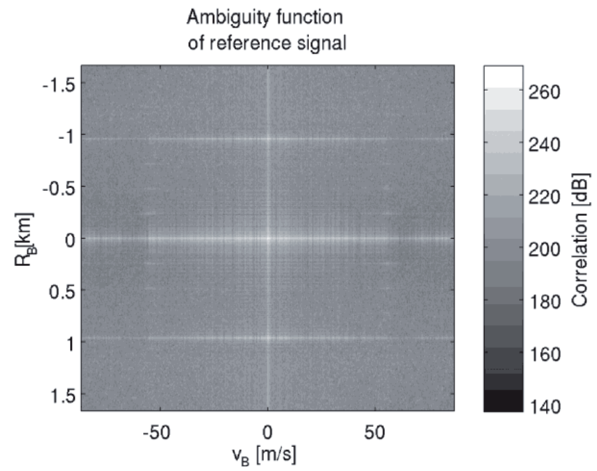

Fig. 6. Ambiguity function of reference signal. Horizontal axis velocity [m/s], vertical axis bistatic range [km].

the parameter that describes ratio between number of samples. This corresponds to frames from a given transmitter and number of all samples in the reference signal. The duty factor can be defined as:

$$F_u = \frac{N_{AP}}{N_{ALL}} \qquad (9)$$

where F_u – duty factor N_{AP} – number of samples that corresponds to frames from a given transmitter, N_{ALL} – umber of all samples in the reference signal.

The cross-section from the crossambiguity function for zero range and for different duty factors is presented in Fig.7. One can see that the peak in crossambiguity function becomes clearly visible and is higher than side peaks for duty factor larger than 0.21.

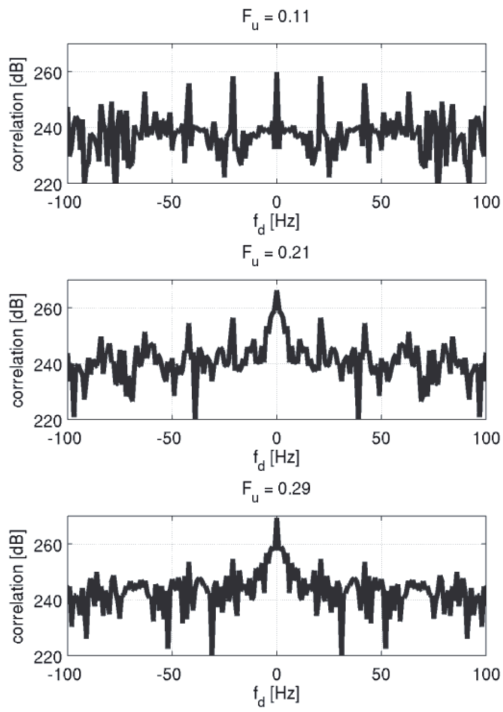

Fig. 7. Slice of the crossambiguity function of reference non separated signal with different duty factor F_u.

The impact of the low duty factor has been also analyzed. In Fig. 8 we can see the separated reference signal–packets corresponding to a single transmitter are selected from the received signal. The duty factor was very low - below 0.1. The crossambiguity function presented in Fig. 9. shows very low quality in case of low duty factor – the sidelobes are very high, and no clear peak is visible.

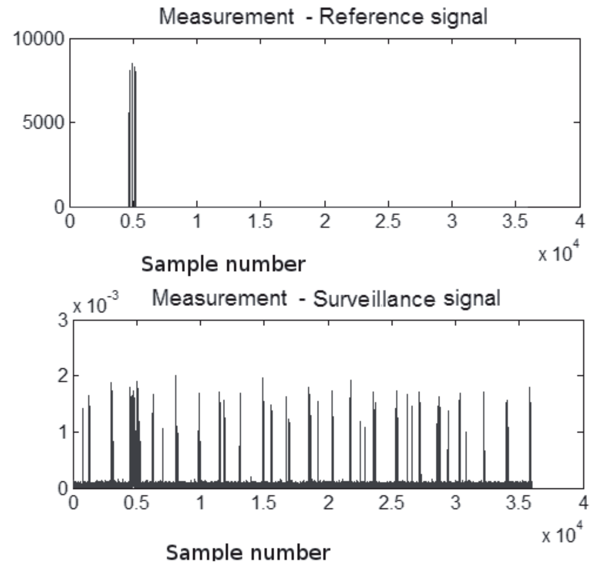

Fig. 8. Measured signals – horizontal axis sample number, vertical axis – signal amplitude [mV]. Upper plot reference signal with low duty factor. Lower plot – sample of surveillance signal.

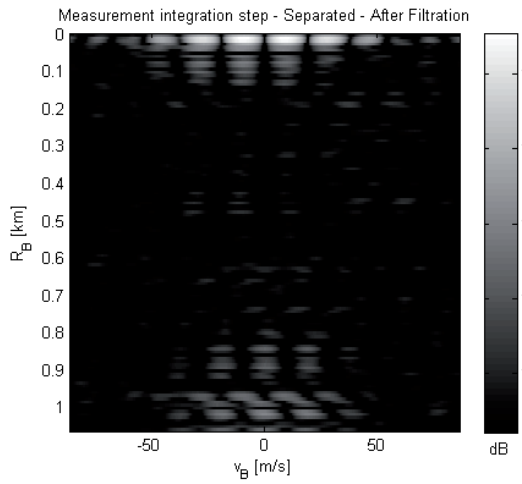

Fig. 9. Radar image based on the separated signal from one of the AP' with very low duty factor and the surveillance signal. Horizontal axis – velocity [m/s], vertical axis bistatic range [km]. Both signals are presented in Fig. 8. Lattice filtering has been applied.

In radar systems with the continuous illumination the main lobe width of the crossambiguity function in the velocity dimension is inversely proportional to integration time and sidelobes can be controlled by an appropriate time window. In WIFIRAD case the illuminating signal is a packet transmission which is equivalent to continuous signal with a binary window (series of rectangles with random length and occurrence). This windowing effect impacts the crossambiguity function. Its impact has been analyzed and discussed in [4] and a method of removing the Doppler sidelobes using CLEAN algorithm was presented in [11], [13].

3.2 Power Budget Analysis

In order to determine area of the possible target detection a power budget analysis has been performed. The simplified bistatic scenario is shown in Fig. 4 where single WIFI AP illuminates target. The direct reference signal comes from AP and its power consumption is not a subject of the power analysis.

Power density of the signal at the distance of target (P_{sdt}) can be stated as:

$$P_{\mathrm{sdt}} = \frac{P_{\mathrm{AP}} G_{\mathrm{AP}}}{4\pi R_1^2} \tag{10}$$

where P_{AP} is the power radiated by AP [W], G_{AP} is the AP antenna gain [unit less], R_1 is the distance from AP to target [m].

The signal emitted by AP illuminates the target and then is reflected in the direction of the radar. The power of the reflected signal depends on bistatic radar cross-section (RCS) which is target unique property. The power density of the reflected signal at the radar side is given by the following equation:

$$P_{\mathrm{sdr}} = P_{\mathrm{sdt}} \frac{\mathrm{RCS}}{4\pi R_2^2} \tag{11}$$

where P_{sdr} is power density of the reflected signal, P_{sdt} is power density of signal at the distance of the target [W/m^2], R_2 is the distance from the target to the radar [m], RCS is the radar cross section of the target [m^2].

The power received by the radar (P_{r}) is given by the formula below:

$$P_r = P_{\mathrm{sdr}} \frac{G_R \lambda^2}{4\pi} \tag{12}$$

where G_{R} is the radar antenna gain, λ is the wavelength [m].

The minimum detectable RCS for the passive radar is calculated by the following formula:

$$\mathrm{RCS}_{\mathrm{min}} = \frac{(4\pi)^3 R_1^2 R_2^2 P_{\mathrm{min}}}{P_{\mathrm{AP}} G_{\mathrm{AP}} G_R \lambda^2} \tag{13}$$

where P_{min} is minimal detectable signal power, expressed as:

$$P_{\mathrm{min}} = \frac{k\, T_0 F_n D_0}{T_i} \tag{14}$$

where T_i is the integration time [s], F_n is the receiver noise factor with losses (6.5 dB in presented case), D_0 is the minimum detectable signal to noise ratio, k is Boltzmann's constant, T_0 is the reference temperature [K].

It is necessary to remember that the signals emitted by the AP are not continuous in time so the mean emitted power depends on the duty factor and the value of P_{AP} in (9) must be multiplied by current transmitter duty factor, which describes the ratio of time of active transmission integration time. Also in real life scenario it is important to take into account losses generated by the loss-elements (like wires, connectors, etc.). With that in mind the final formula for minimal RCS is:

$$\mathrm{RCS}_{\min} = \frac{(4\pi)^3 R_1^2 R_2^2 \mathrm{k}\, \mathrm{T}_0 F_n D_0 L_{\mathrm{sys}}}{P_{\mathrm{AP}} F_u G_{\mathrm{AP}} G_R \lambda^2 \tau} \tag{15}$$

where L_{sys} are system losses, F_{u} is duty factor .

The prediction of the passive radar detection range was calculated assuming that RCS of the Cessna C208 airplane is equal to 5 m^2 [2].

In a multistatic scenario minimum detectable RCS can be defined as RCS that provides target visibility for all bistatic pairs. In other words it would be the maximal value of $\mathrm{RCS}_{\min}$ for each point in the plane. Multistatic $\mathrm{RCS}_{\min}$ for assumed position of WIFIRAD and AP's at the Chrcynno Airfield is presented in Fig. 10. The white color in Fig. 10 means that the minimal detectable RCS is below 1 square meter. The 0 dBsm target should be detected at the distance of 1 km, while Cesna should be detected up to 1.5 km. Those results convinced the authors that the experiment can be successfully performed. In theory it would be possible to detect target with RCS equal to 5 m^2 on Chrcynno Airfield runways.

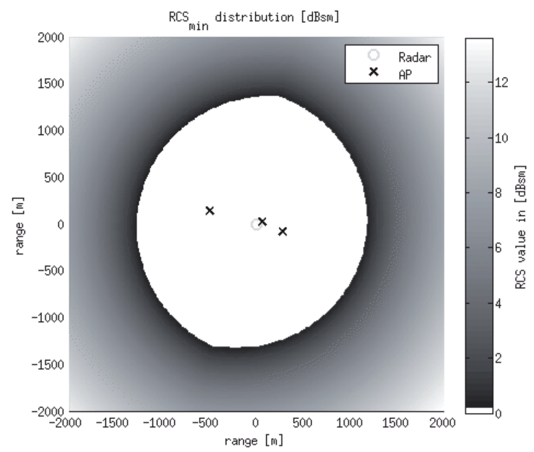

Fig. 10. $\mathrm{RCS}_{\min}$ distribution on Chrcynno airfield. x stands for wireless AP and o stands for WIFIRAD. White region shows area where $\mathrm{RCS}_{\min}$ is below 1 m^2.

3.3 Target Localization in Multistatic Passive Radar

In general situation during the target localization in the bistatic passive radar, the ellipsoid is created (3Dimensional situation). That ellipsoid indicates all the possible target locations, because the difference of times of propagation between reference and surveillance signal is constant for the ellipsoid. In 2D scenario instead of ellipsoid there is an ellipse of the possible target location. In our experiment (airfield can be simplified as 2D scenario) there are 3 transmitters and 1 receiver, so there are 3 bistatic ellipses. These 3 ellipses should intersect in 1 point giving the final position of the target in 2D scenario [14]. Obviously in the real life scenario measurements are made with error that is caused by radar range resolution (range cell size is 7.5 m).

The precise Cartesian coordinates of the target can be calculated in passive radar using two approaches: an angle measurements or a bistatic distance measurement. While the angle measurements are more complicated than the bistatic range measurements, the method used in the experiment was based on finding the ellipses intersection point. It should be noted that in the experiment we have three bistatic pairs - radar and AP. Each such a pair forms a bistatic ellipse which focal points are the positions of the radar and AP. This in fact creates the multistatic scenario with 3 ellipses with one common focal point (position of the radar). These ellipses will have one point of intersection (as described in [14]) which indicates the target position.

The precision of the target position measurement highly varies with the relative location between target, receiver and transmitters. In case when two ellipses intersect with a low angle (tangents in intersection point have a small angle), the position of a target will be estimated with a large error. The intuition suggests that the intersection of all 3 ellipses should occur with large angle to minimize that error. In the real life environment for passive radar there is a little possibility to change the system situation. The area where the target was expected had been known before the experiment was performed. The position of the AP's and the radar has been selected in such a way to avoid possible problems with a low angle of the ellipses intersection point.

The final position of the AP stations and radar has been presented in Fig. 11 as well as the ellipses (their focal points are AP's and WIFIRAD). Their intersection point indicates a target – which is an airplane moving on the runway (taxing). One should note that other intersection points that do not belong to all three ellipses are the ghost targets that we are not interested in.

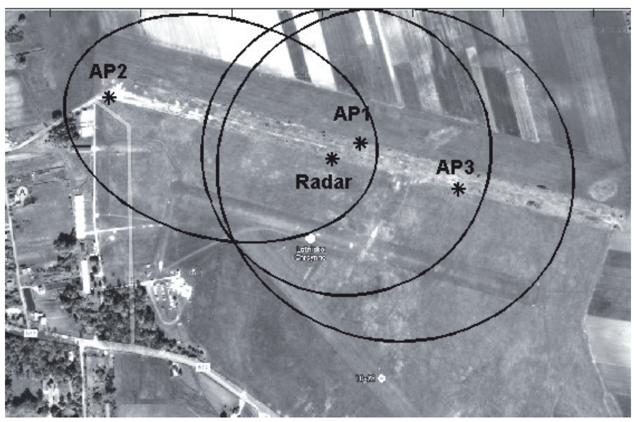

Fig. 11. Ellipses on Chrcynno Airfield with the indication of the target position on the runway (intersection point).

As long as we consider only 2-dimensional case, velocity v can be calculated using two bistatic velocities (obtained from two pairs of transmitter and receiver) from the following system of equations:

$$\begin{aligned} v \cdot u_1 + v \cdot u_2 &= \mathrm{v}_{B1} \\ v \cdot u_3 + v \cdot u_4 &= \mathrm{v}_{B2} \end{aligned} \qquad (15)$$

where v is the velocity vector, v_{B1} is the bistatic velocity obtained from the first pair of the transmitter and receiver, v_{B2} is the bistatic velocity obtained from the second pair of the transmitter and receiver, u_3 and u_4 are versors similar to u_1 and u_2 from the second pair of Rx - Tx.

In that calculations it has been assumed that the position of an object is known, determined from the intersection of ellipses. Knowing this and the positions of Rx and Tx, versors u_1 and u_2 can be determined. The vector v can be expressed as:

$$v = \begin{bmatrix} v_x \\ v_y \end{bmatrix}. \qquad (16)$$

The system of equations (15) can be expressed as a matrix equation as follows:

$$\begin{bmatrix} u_{1x}+u_{2x} & u_{1y}+u_{2y} \\ u_{3x}+u_{4x} & u_{3y}+u_{4y} \end{bmatrix} \cdot \begin{bmatrix} v_x \\ v_y \end{bmatrix} = \begin{bmatrix} v_{B1} \\ v_{B2} \end{bmatrix} \qquad (17)$$

where: u_{kx} is versor u_k projection to X-axis in Cartesian coordinate system, u_{ky} is versor u_k projection to Y-axis in Cartesian coordinate system, k = 1, 2, 3, 4, v_x is the velocity of the target on X axis direction in Cartesian coordinate system, v_y is the velocity of the target on Y axis direction in Cartesian coordinate system.

$$U = \begin{bmatrix} (u_1+u_2)^T \\ (u_3+u_4)^T \end{bmatrix} = \begin{bmatrix} u_{1x}+u_{2x} & u_{1y}+u_{2y} \\ u_{3x}+u_{4x} & u_{3y}+u_{4y} \end{bmatrix}. \qquad (18)$$

Solution of this system of equations can be stated as:

$$1 \,|\cdot \vec{v} = \begin{bmatrix} u_{1x}+u_{2x} & u_{1y}+u_{2y} \\ u_{3x}+u_{4x} & u_{3y}+u_{4y} \end{bmatrix}^{-1} \cdot \begin{bmatrix} v_{B1} \\ v_{B2} \end{bmatrix} \qquad (19)$$

where 1 | is identity matrix

After solving that equation the target velocity can be obtained.

4. Experiment Description

The experiment has been performed near village Chrcynno on the grass airfield (CHR1) which is used by paratroopers. All the presented results of the experiment in this paper refer to situation when Cessna C208 airplane is moving on the ground (taxing - moving after landing or accelerating before take-off) – 2D scenarios. It was expected to detect target in the air but due to sensitivity of the recording devices it was not possible. Usage of high gain omnidirectional antennas (radiating radio wave power uniformly in all directions in one plane), allowed us to obtain the higher ranges. Unfortunately it also made it difficult to perform a 3-dimensional localization. The WIFI network was designed and built for the experiment needs. The following network components were used: 3 WIFI nodes using MikrioTik RouterBoard 433AH and MikrioTik RouterBoard 600. To each Router Board a WIFI card with extended sensitivity has been plugged in (RouterBoard-R52Hn). Each WIFI node has been connected using 17 dBi antenna via 1.5 meter cable (H155). WIFI traffic used in the experiment was generated by MikrioTik bandwidth test application (client-server). Also a small amount of ICMP traffic between WIFI network nodes has been added. The traffic details have been shown in Tab. 1.

Type of Packets	Between NODES	Throughput
UDP	3-1	UDP 256Kbps in both directions
TCP	2-1	TCP, 1Mbps in both directions
ICMP	1-2 and 1-3	ICMP 22.4Kbps each flow

Tab. 1. WIFI network traffic used in Chrcynno experiment.

The National Instruments PXiE-1075 linked with Disk array have been used for data acquisition. Depending on the scenario, the signal was acquired using 17 dBi antenna or 24 dBi directional antenna.

Fig. 12. On the left 17 dBi omnidirectionl antenna, on the right directional 24 dBi antenna.

The experiment has been performed in 31 different scenarios. Scenarios differ between each other by:

- the antenna type and configuration used for signal acquisition by WIFIRAD,
- different plane position on the airfield – taxing, taking off, landing, approaching the runway,
- plane operating on different runway 106/286 or 136/316,
- length of the recorded measurement.

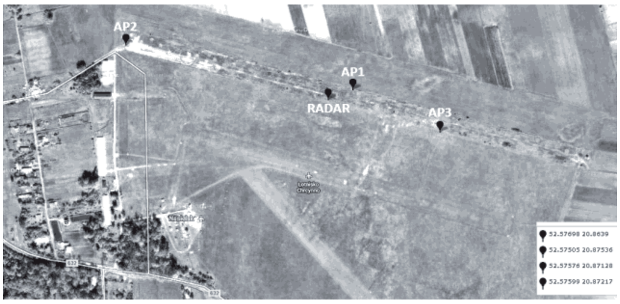

Fig. 13. Position of WIFI AP's and WIFIRAD radar along the damaged concrete runway in Chrcynno. Two grass runways visible on the photo, first 106/286 deg parallel to concrete and the second one inclined 136/316 deg.

In this paper we will focus on plane taking-off from runway on the direction 136/316 deg. and measurement length 20 seconds. In the described scenario omnidirectional antennas were used on the AP's side and the radar as equipped with the directional antennas (antennas shown in Fig. 12). We are using 3 AP's so theoretically the position of the target is defined clearly – only one intersection point of all 3 ellipses [14]. In practice there will occur some measurement errors. In that case it would be necessary to apply more sophisticated localization methods. One of those can be searching for the point that minimizes the distances to all ellipses.

4.1 Data Processing

The architecture of the application used for data processing is presented in Fig. 14.

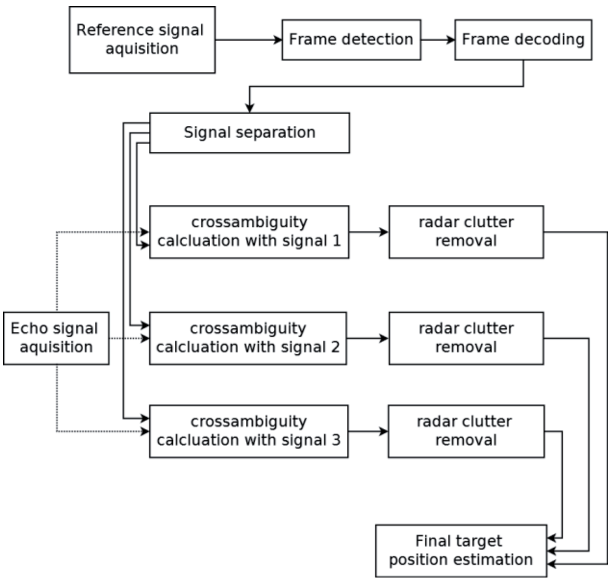

Fig. 14. The architecture of the application for data processing.

The signal was recorded by the NI PXiE signal recorder and then processed off-line in the Matlab environment. At the first step the WIFI frames were detected and extracted from the reference signal. Frame detection algorithm was based on the correlation of reference signal with training sequences (a part of the WIFI FRAME that is always the same on the physical layer for given transmission speed in OFDM modulation). In the next step the signal is decoded and sorted by the MAC source address. MAC source address allows us to distinguish the signal from the different transmitting nodes and separated signals belonging to different transmitters of opportunity. As the result of this step, the reference signal from different transmitting nodes (different illuminators) was formed. These signals are being used for further calculation of the cross-ambiguity function (6). In the next stage, ground clutter was removed using the lattice filters [11], [13] (order of 70).

The result of the processed signal with a visible target can be seen in Fig. 15. It should be noted that without the signal separation (distinction of reference signal to signals belonging to given AP) that was applied in the processing, it was not possible to detect any target at all.

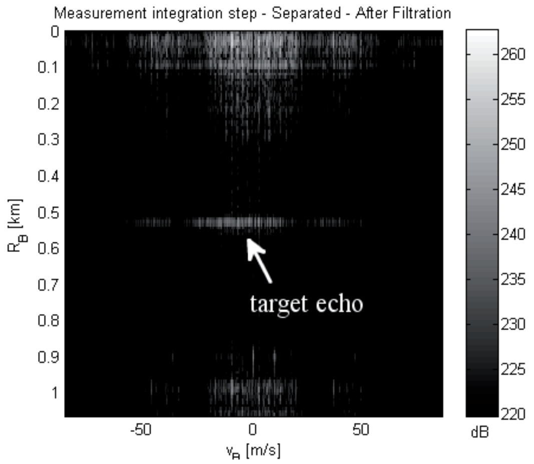

Fig. 15. Echo from Cessna C208 airplane taxing on the grass runway. Horizontal axis: velocity [m/s], vertical axis: bistatic range [km]. Lattice filtering has been applied.

Many various methods of the frame detection have been used and tested in the signal processing. Starting from the simple one, based only on fixed threshold value to more advanced methods with adaptive threshold. Also a CFAR like (Constant False Alarm Ratio) an algorithm for frame detection has been developed and tested. However all these methods had a problem with the frame detection because of the large dynamic scale of the acquired signal (the signal sources were in different distance from the radar). Some frames had a very low level of amplitude in comparison to the ones that were captured from the stronger signal source in the reference channel. The best results (empirically tested - max. number of detected frames in the reference signal) have been obtained by the correlation of the reference signal with a training sequence. This operation provided a spike visible at the beginning of each frame. The CFAR algorithm has been used to detect these spikes. In that way all the starting points of the frames in the reference signal have been found.

4.2 Training Sequence Removal

Because each WIFI FRAME contains so called TRAINING SEQUENCE part of PLCP PREAMBLE

(Fig. 3) which is not changing from FRAME to FRAME, an algorithm has been designed to remove TRAINING SEQUNCES. The purpose behind that action was to remove the repeating parts of the signal to avoid so they will not be correlating between each other and the radar clutter will be much clearer. The training sequence that was removed from each frame is presented in Fig. 16.

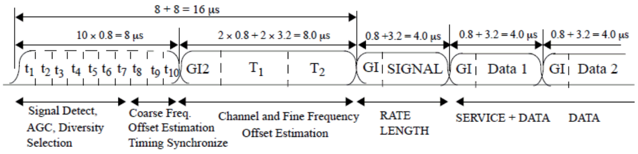

Fig. 16. PHY layer presentation of the OFDM WIFI Frame [12].

After removing the training sequence, the gain at the target area was not large (below 0.5 dB). However the noise reduction from the antenna leakage and in the area around the target has been observed. It shows that there is some potential in removing similar frame octets in each frame.

4.3 Integration Time Impact

The signal processing has been performed with a different integration times to find empirically the most optimal integration time for detecting target (an airplane taking-off from runway that is on the direction 136/316 deg). The following integration times have been used in the data processing: 0.1, 0.2, 0.5, 0.8, 1 second and 2 seconds. The most interesting results are shown in Fig. 17 and Fig. 18.

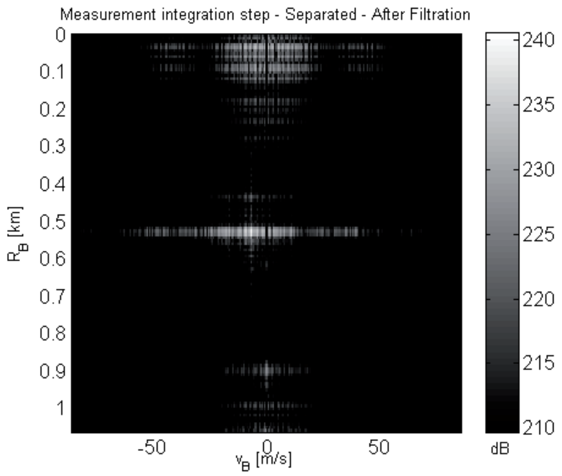

Fig. 17. Radar image for the integration time 0.2 s. Reference signal – AP1. Horizontal axis – velocity [m/s]. Vertical axis bistatic range [km]. Lattice filtration has been applied.

The higher the integration time the more energy is accumulated in the processed signal, however, during that integration time the target was moving so the energy was spread. However at some integration time value it can be observed that longer integration does not significantly increase the echo from the target. The distance between the noise floor and the target echo is about 20 dB and does not change much with the integration time. From the presented data it can be observed that the trade-off between Doppler resolution, signal power from target echo and integration time is around 1 second and this is the integration time that was used in the processing of the experiment data.

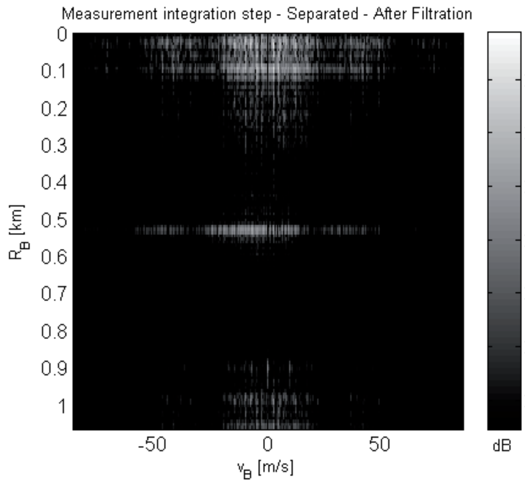

Fig. 18. Radar image for the integration time 1 s. Reference signal – AP1. Horizontal axis – velocity [m/s]. Vertical axis bistatic range [km]. Lattice filtration has been applied.

Fig. 19. Target Cessna C208 airplane taking off from the runway on the direction 136/316 in the 12th second of measurement – no optical zoom used.

Cessna C208 airplane has been presented in Fig. 19. Photo was taken in 12th second of the measurement and it corresponds to time of measurement of radar clutter presented in Fig. 17 and Fig. 18. Camera that was taking picture was located at the radar position without any optical zoom.

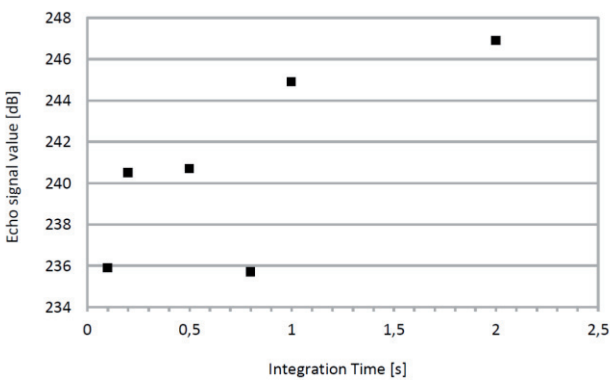

Fig. 20. Target echo strength (arbitrary dB scale) in function of integration time.

5. Conclusions

The results of the experiment prove that the target detection is possible using a WIFI network nodes as the illuminators of opportunity in multistatic configuration. The target can be not only a car [5] but, as it is shown in that paper also a small airplane. Before the experimental work started, the research in the following areas had been done, namely: finding the minimal RCS and its distribution in radar environment, finding the tradeoff between the target detectability and the integration time, evaluating utilization factor value vs its impact to crossambiguity function, finding practical method for frame detection.

1. Finding target on the radar clutter results
2. Checking if the removal of a training sequence from the frames in the reference signal is beneficial

All of the research goals are described in the details in this paper. Further research will be focused on finding other interesting targets that could be detected and tracked by WIFIRAD as well as on improving radar ability to detect the objects and/or the noise reduction. The target tracking will be also a subject of our research investigation in the WIFIRAD project.

Acknowledgements

This work has been partially supported by the National Center for Research and Development under the project no. DOBR/0043/R/ID1/2012/03 "Development of passive radar system for air defense missile systems".

References

[1] SKOLNIK, M. I. *Radar Handbook.* 3rd ed. 2008 ISBN-10: 0071485473

[2] COMMUNICATIONS RESEARCH CENTRE *Radar Detectability of Light Aircraft.* U.S department of Commerce National Technical Information Service, AD-A029 262, April 1976.

[3] RZEWUSKI, S., KULPA, K. System concept of WIFI based passive radar. *International Journal of Electronics and Telecommunications,* 2011, vol. 57, no. 1, p. 447–450.

[4] KULPA, K., RZEWUSKI, S., GAJO, Z., MALANOWSKI, M. Concept of multistatic passive radar based on wireless packet communication systems. In *Proceedings of 2011 IEEE CIE International Conference on Radar*. Chengdu (China), Oct. 2011, p. 149-152. DOI:10.1109/CIE-Radar.2011.6159497.

[5] RZEWUSKI, S., WIELGO, M., KULPA, K., MALANOWSKI, M., KULPA, J. Multistatic passive radar based on WIFI results of the experiment. In *Proceedings of 2013 IEEE CIE International Conference on Radar*, Adelaide (Australia), September 2013, p. 230-234. 09/2013, DOI: 10.1109/RADAR.2013.6651990

[6] QIFAN PU, SIDHANT GUPTA, SHYMANATH GOLLAKOTA, SHWETAK PATEL Whole-home gesture recognition using wireless signals. In *The 19th Annual International Conference on Mobile Computing and Networking*, 2013.

[7] PIETROSEMOLI, E. *Long distance WIFI trial.* In *International Summit for Community Wireless Networks.* Columbia, 2007. [Online] Available at http://www.slideshare.net/1ereposition/long-distance-WIFI-trial

[8] GASHINOVA, M., DANIEL, L., HOARE, E., KABAKCHIEV, K., SIZOV, V. Forward scatter radar mode for passive coherent location systems. In *Proceedings of 2013 IEEE CIE International Conference on Radar*. Adelaide (Australia), September 2013, p. 235-239. DOI: 10.1109/RADAR.2013.6651991

[9] KRYSIK, P., KULPA, K., BACZYK, M., MASLIKOWSKI, L., SAMCZYNSKI, P. Ground moving vehicles velocity monitoring using a GSM based passive bistatic radar. In *Proceedings of 2011 IEEE CIE International Conference on Radar*. Chengdu (China), Oct. 2011, p. 781-784. DOI:10.1109/CIE-Radar.2011.6159657.

[10] MALANOWSKI, M., KULPA, K., MISIUREWICZ, J. PaRaDe - PAssive RAdar DEmonstrator family development at Warsaw University of Technology. In *Microwaves, Radar and Remote Sensing Symposium*. Kiev (Ukraine), 2008, p. 75-78. DOI: 10.1109/MRRS.2008.4669549

[11] KULPA, K., CZEKALA, Z. Masking effect and its removal in PCL radar. *IEE Proceedings of Radar Sonar and Navigation*, June 2005, vol. 152, no. 3, p. 174-178.

[12] IEEE, IEEE802.11a-1999 part 11: *Wireless LAN Medium Access Control (MAC) and Physical Layer (PHY) specifications*. IEEE, 1999.

[13] KULPA, K., CZEKALA, Z. Ground clutter suppression in noise radar. In *Proceedings of International Conference RADAR*. Toulouse (France), 2004, p. 236.

[14] MALANOWSKI, M., KULPA, K. Two methods for target localization in multistatic passive radar. *Transactions on Aerospace and Electronic Systems*, 2012, vol. 48, no. 1, p. 572-580. IEEE Log No. T-AES/48/1/943634.

[15] HOWLAND, P. E., MAKSIMIUK, D., REITSMA, G. FM radio based bistatic radar. *IEE Proceedings of Radar, Sonar and Navigation*, June 2005, vol. 152, DOI 10.1049/ip-rsn:20045077.

[16] GRIFFITHS, H. D., BAKER, C. J., PAPOUTSIS, I. Passive coherent location radar systems. Part 2: Waveform properties. *IEE Proc. Radar, Sonar and Navigation*, June 2005, vol. 152, no. 3, p. 153–159.

About Authors …

Stanisław RZEWUSKI was born in 1981. He received his M.Sc. from Applied Mechanics in 2006 and the second

M.Sc from Telecommunication in 2008. Both degrees have been received from the Warsaw University of Technology. His research interests include passive radars, telecommunication systems and space technologies.

Maciej WIELGO was born in 1988. He received his B.Sc. from Computer Science and Telecommunication in 2012. His research interests include radars, telecommunication systems and signal processing.

Karol KLINCEWICZ was born 1988. He received his B.Sc. from Electronics and Computer Engineering in 2012. His research interests include signal processing, radiolocation and signal detection.

Krzysztof KULPA was born in 1958. He received his M.sc and Ph.D. from the Warsaw University of Technology 1982 and 1987, respectively. His research interests include signal processing, SAR and passive radars.

Mateusz MALANOWSKI was born in 1980. He received his M.Sc., Ph.D. and D.Sc degrees in Electrical Engineering from the Warsaw University of Technology, Warsaw, Poland, in 2004, 2009, and 2013 respectively. His research interests are radar signal processing, target tracking, passive coherent location, synthetic aperture radar and noise radar.

Łukasz PODKALICKI was born in 1985. His research interests include telecommunication and security systems.